



Characterization of northeast Greenland cave sediments

Johannes TISCHLER¹, Paul TÖCHTERLE¹ and Gina E MOSELEY¹

¹Institute of Geology, University of Innsbruck, Innrain 52, 6020 Innsbruck, Austria.
E-mail: gina.moseley@uibk.ac.at

Abstract: Clastic sediments deposited in caves are useful archives of past hydrological and environmental conditions. Here we report the results of investigations into three samples of clastic sediments collected from caves in northeast Greenland. The samples have a mineralogical composition dominated by calcite, dolomite and quartz. Two of the samples are homogenous silts, whereas the third sample is laminated with couplets that begin with a pale grey silt, and fine upwards to a darker clayey-silt that is higher in organic carbon. All sediments were deposited in calm to stagnant conditions though the laminae in the one sample indicate pulsing in the depositional process, possibly caused by waxing and waning of an internal ice plug or external glacier.

Received: 25 April 2020; *Accepted:* 09 May 2020.

Clastic sediments found in caves are important archives that record both the cave's history and the external climate and environment at the time of deposition (Ford, 2001; Sasowsky, 2007). Due to their geomorphological characteristics, caves commonly serve as sediment traps whereby they catch material formed through various processes operating within the landscape, preserve it, and protect it from external weathering. Where it is possible to establish accurate chronologies of deposition, caves provide important settings for studying Earth's past climate and environment.

Clastic sediments are classified either as autochthonous or allochthonous (White, 2007). Generally they are formed by particles that are moved mechanically and deposited, and are differentiated from one another based on particle diameter. On the international scale (ISO 14688-1), anything smaller than 2µm is classified as clay, irrespective of mineralogy. Particles between 2 to 63µm form silt, from 63µm up to 2mm they are called sand, between 2 to 63mm is gravel, cobbles are sized 63 to 200mm, and boulders are larger than 200mm. Using the information on grain-size distribution in a particular deposit, it is possible to derive the degree of sorting of the sediments, which in turn can be used as an indicator of the mode of transport (water, ice, or wind) (Ford, 2001). According to Sun *et al.* (2002), every method of transportation leaves its mark on the grain-size distribution of the forming sediment. Aeolian sediments, for example, consist of small dust particles about 2.6µm in size, which are suspended in the air, as well as bigger material with a grain-size between 25–73µm. For fluvial sediments, the transported material is divided into a saltation and a suspension component. The latter component shows a grain-size distribution in the range of 10–15µm (poorly sorted) and the saltation material varies between 200–400µm (well sorted) (Sun *et al.*, 2002). Alongside the diameter, the roundness of the particles may also be used as an indicator of the distance of travel (Ford, 2001).

Autochthonous sediments consist of material formed within the cave environment, e.g. breakdown and other local material such as small insoluble particles that are residual after solution of the bedrock, which is generally limestone. Most commonly, such insoluble particles are clay-sized and contain a variety of compounds released from the surrounding rock (Ford, 2001).

In contrast, allochthonous material originates from outside the cave and can be transported by water or wind. Additionally, in cave entrance areas, 'entrance talus' builds up from a variety of material including weathered rock from above the cave, weathered material that is transported into the cave, and plant material (White, 2007).

Transport and deposition of sediments within a cave occurs through a variety of processes. Sediments that are washed into a cave, for example by a sinking stream, commonly contain unconsolidated material such as alluvial sediments, volcanic ash, or glacial in-wash. This material may be transported in two ways (White, 2007), with the first being transportation in suspension. Depending upon the hydrological energy, sediments of different sizes may be carried in suspension by the stream. The second mode of transportation happens at the contact between water and the streambed where shear forces drag loose material along it (White, 2007). Inside a stream cave, many potential resting places exist for sediments, which together need to be examined and put in relation to the specific drainage system operating in the cave. Accumulation of gravels and cobbles may indicate a powerful stream event, whereas deposition of sand occurs whenever the stream velocity is reduced. Sediments in caves can thus be used to help reconstruct a cave's hydrological history because indicators of environmental changes may be documented in the sediments. Sediments found in caves are commonly deposited in layers with a thickness from millimetres to centimetres. The layers contain evidence of changes to the depositional process over time (Ford, 2001). Changes in the mineral content can also be interpreted to provide details of the potential source areas of the clay. Sediments may additionally be transported and deposited by ice. Deposition takes place when the ice melts and the resulting water transports particles that were trapped on top, inside, or pushed ahead of the ice. This process can take place at different scales, ranging from isolated ice bodies inside a cave chamber to regional glaciation of karst terrains.

Results of the first investigations into clastic sediments found in caves in northeast Greenland are reported here. The study was undertaken as part of a one-semester Bachelor thesis at the University of Innsbruck, Austria.

Field sites

Sediments were studied from three caves in northeast Greenland. The caves are within two tributary valleys situated on the southern side of the c.2.5km-wide Grottedal valley (Fig.1). Grottedal itself trends northwest–southeast, with the valley floor dropping from c.400 to 200m above sea level (a.s.l.) respectively. At its southeastern end, Grottedal joins the 10km-wide Vandredalen, which drains from Centrumso, an over-deepened 20km-long, 4km-wide glacial lake with its surface at 98m a.s.l. (Krisley, 1960) (Fig.1). Presently the caves are c.55km from the ice margin. The three caves studied here are referred to as “Lemming Cave” (Narlumukaap Qaarusussuaq; Lat: 80.39°, Long: –21.82°), “U-Shaped Cave” (U-Tut Ilusilik Qaarusussuaq; Lat: 80.38°, Long: –21.73°) and “The Tube South” (Lat: 80.38°, Long: –21.73°), though note that these are not official names approved by the Language Secretariat of Greenland (oqaasileriffik.gl/place-names). All the caves are located within limestones of the c.320m-thick Odins Fjord Formation (Smith and Rasmussen, 2020).

Lemming Cave is located at c.526m a.s.l. on the northern side of a sharp s-bend in a steep-sided, narrow (c.100m-wide) canyon (Fig.1). The canyon floor outside the cave is c.510m a.s.l., and in July 2019 it was free of running surface water. A cave description and survey are provided by Moseley *et al.*, (2020) but in summary, the cave entrance is found at the top of a steep scree-slope that extends to the canyon floor. The cave, which is c.54m long and relatively horizontal from the top of the entrance slope, includes a c.15m-long northeast–southwest-trending entrance passage, from which the way on is presently blocked by ice. At the top of the entrance slope, a c.10m-long hands-and-knees crawl heads off to the east and reaches a small, c.4m-high, aven (Moseley *et al.*, 2020). The crawl continues for a further c.10m, finally ending in a small, c.2m diameter, chamber dubbed ‘The Spaceship’, which is completely blocked by ice devoid of air inclusions. Hanging from the bottom of the ice is a c.15cm-diameter cobble (Fig.2a). Fragments of laminated sediments were discovered in this final chamber beneath the ice plug (Fig.2a) and several hand specimens were sampled (LC-S1) for further investigation. The sediments covered an area c.0.5m by 0.5m. Whereas the total thickness of the sediments remains unknown, sample LC-S1 has a thickness of approximately 10cm.

U-Shaped Cave is situated in the next valley to the east (Fig.1). It has two large entrances (c.13m × 10m and c.8m × 5m) located at c.533 and c.530m a.s.l. (Moseley, 2016), and thus is at a comparable elevation to Lemming Cave. In contrast to Lemming Cave, however, the valley bottom is at c.350m a.s.l. beneath U-Shaped Cave. Therefore U-Shaped Cave is perched some 180m above the valley floor. The cave has formed along the contact between beds of pale grey and dark grey limestone. Its floor is covered with sediment and breakdown blocks, and ice can be found as thin layers on the lower side walls.

The sediments collected in this cave (GD4-S1) are not laminated; they were collected simply by scraping powders into a sample bag from close to the part with the lowest ceiling height in the centre of the cave (Fig.2b) (Moseley *et al.*, 2020).

The Tube South (Fig.2c) is a short horizontal cave located at 452m a.s.l. in the same valley as U-Shaped Cave (Fig.1). This ice-free cave has a small entrance, about 1.5m wide and 0.9m high, with a length of only 3.5m. Fracture-filling calcite deposits and fine-grained sediment were reported (Moseley, 2016). Like the deposits in U-Shaped Cave, the sediments in this cave (GD2-S1) are not laminated and were collected by scraping material from the floor into a sample bag.

Analytical methodology

Macro- and microscopic investigations

All samples were investigated both macroscopically and microscopically. The laminated sediments found in Lemming Cave (LC-S1) were investigated using a VHX-5000 digital camera system from Keyence, which has several objectives and is operated directly by its own software programme, allowing editing and modification of the pictures. Using the VHX-5000, it was possible to measure the thickness of the individual layers and determine the stratigraphy of the sample.

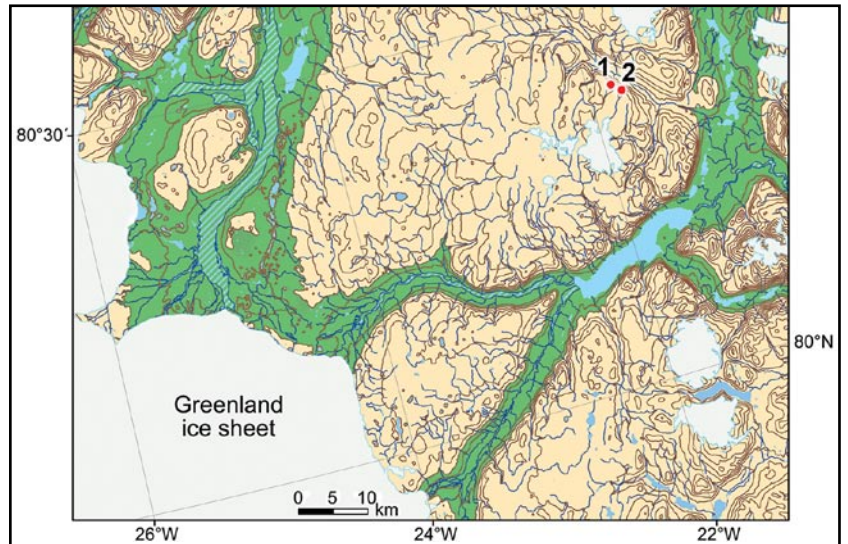


Figure 1: Topography of the study area, showing the edge of the Greenland ice sheet and three cave locations. Site 1 is Lemming Cave; Site 2 is U-Shaped Cave and The Tube South. [Contains data from Styrelsen for dataforsyning og effektivisering, “Topografiske kort i målforhold 1:250.000. Datasættet er produceret i perioden 1990–2000.”, May 2020.]



Figure 2a: Ice plug in Lemming Cave, with (LC-S1) laminated sediments beneath. [Photo: Robbie Shone.]



Figure 2b: Sample GD4-S1 collected from U-shaped Cave. [Photo: Robbie Shone.]



Figure 2c: Entrance to The Tube South. [Photo: Robbie Shone.]

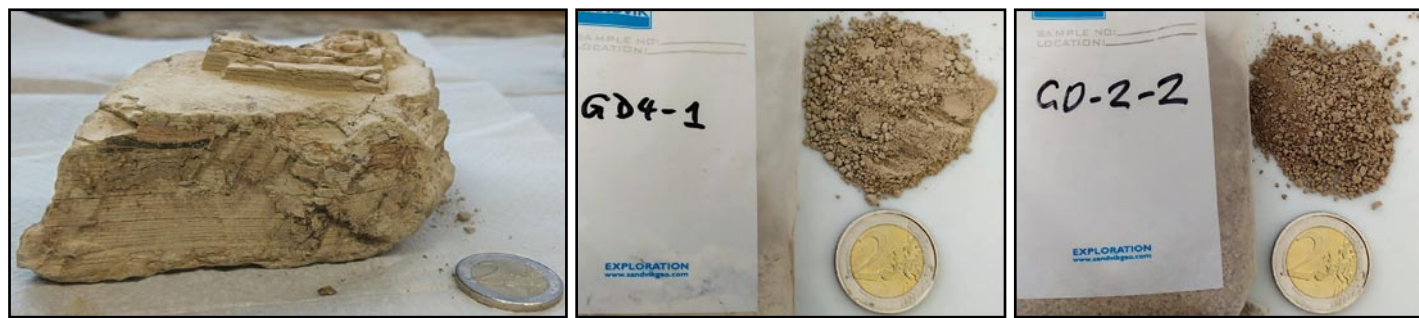


Figure 3: 3a (Left): Sample LC-S1; 3b (Centre): Sample GD4-S1; 3c (Right): Sample GD2-S1 [relabelled]. Scale: 2-Euro coin (diameter 26mm).

Grain-size analysis

Samples were analysed for grain-size using a Malvern Instruments Mastersizer 3000. LC-S1 was split into two sub-samples broadly containing pale (LC-S1_{pale}) and darker (LC-S1_{dark}) material, whereas GD4-S1 and GD2-S1 were analysed in bulk. Where possible, samples were measured in a dry and wet-suspended state. For some samples, it was necessary to pre-treat them by putting them in suspension for 12 hours to break apart agglomerations. Samples were run by using standard operating procedures configured by Marcel Ortler, University of Innsbruck.

To break agglomerations apart more completely, so that original particle sizes could be determined, an ultrasonic bath was used, set at 15% intensity for 60 seconds. The LC-S1_{dark} sample was an exception, requiring ultrasound at 80% intensity for 200 seconds.

Carbon analysis

Carbon content of the samples was investigated to determine the organic and inorganic carbon ratio. Two sub-samples from each sample were ground finely in a mortar, and one aliquot was pre-treated with 20–30ml 5% HCl. After three hours, all beakers were decanted, and rinsed twice with de-ionised water to remove HCl residue. The carbon content of each sample was measured in an Eltra CS-580A Carbon-Analyzer. 200mg samples placed in a ceramic crucible were combusted in the analyzer at 1350°C. Released CO₂ was measured by infrared absorption and compared to pure synthetic CaCO₃ as a reference material to determine the C content of the sample (%wt C). Because it was not possible to sample enough LC-S1_{dark}, a bulk sample (LC-S1_{bulk}) containing proportions of both pale and dark material was analysed.



Figure 4: Microscopic investigation of LC-S1 reveals alternating pale and dark layers and upward fining.

	LC-S1 _{pale} dry	LC-S1 _{pale} wet	LC-S1 _{dark} dry	LC-S1 _{dark} dry ₂	GD2-S1 dry	GD2-S1 wet	GD4-S1 dry	GD4-S1 wet
Clay: <2µm (%)	14.3	15.8	49.8	48.4	16.5	18.7	7.8	7.4
Silt: 2–63µm (%)	85.7	84.2	50.2	51.5	83.5	78.4	92.0	92.0
Sand: >63µm (%)	0.02	0	0.0002	0.05	0.06	2.9	0.2	0.6

Table 1 (above): Results of the grain-size analysis.

X-ray diffractometry (XRD)

To determine mineralogical phases within the deposits, 1–2mg sediment samples, homogenized by grinding in an agate mortar for 5 minutes, were analysed using XRD at The University of Vienna. The principle of XRD is that each sample is irradiated with X-rays; each different mineralogical phase has a slightly different crystal lattice that causes the rays to be diffracted at different angles. The rays and their intensities are measured to produce a diffractogram wherein the peaks are interpreted to identify mineral components within the sample.

Results

Macro- and microscopic investigations

Macroscopic investigation of the three samples shows that LC-S1 is laminated whereas GD2-S1 and GD4-S1 are not (Figs 3a–c). Macroscopically, LC-S1 displays layers in the micrometre to millimetre scale, with couplets alternating between darker and paler colours. In a 27mm-thick sample of LC-S1, a total of 23 couplets were counted, and in a separate fragment, 36 couplets in 39mm. Microscopic investigation of LC-S1 showed that the coarser-grained pale material fines upwards to the darker layer (Fig.4). These pale-to-dark lamina couplets are separated by sharp contacts. The paler layers are between 1.0mm and 1.9mm thick, with an average thickness of 1.4mm (n=10). In contrast, the darker layers are substantially thinner, with an average thickness of just 0.1mm.

Grain-size analysis

The results of the grain-size analysis are presented in Table 1 and the key features summarized here. Each sample shows comparable results for its wet and dry fraction; however, the composition of the three samples is quite variable. All the samples contain clay and silt fractions with sand being virtually negligible. The dominant fraction in GD2-S1, GD4-S1 and LC-S1_{pale} is silt. In the case of GD2-S1 and LC-S1_{pale}, they are most comparable to one another, whereas GD4-S1 displays c.7% more silt and c.7% less clay than GD2-S1 and LC-S1_{pale}. In contrast to these three comparatively similar samples, LC-S1_{dark} has a rather different ratio of silt to clay comprising roughly 50% of each fraction. The clay content of LC-S1_{dark} is therefore three to six times greater than in the other samples.

Carbon analysis

The results of the carbon analysis (Table 2) show that the carbon contents of the samples are approximately the same at c.8% total carbon and c.0.2 to 0.3% organic carbon. Inorganic carbon was of the order of 7.5 to 8.0%, making up most of the carbon content of the samples. When comparing the bulk and pale samples of LC-S1, the results show that the bulk sample has a slightly higher organic carbon content (0.31%) as compared to the pale layer (0.16%). Because the bulk sample contains both pale and dark material, the higher organic carbon content of the bulk sample probably originates in the dark layers.

	Carbon content (%)				
	Non-acid treated		Acid treated		
Calcite Standard	12.05	12.01	11.97	12.07	12.02
GD2-S1	7.27	7.26	7.27	0.28	–
GD4-S1	8.13	8.18	–	0.29	0.27
LC1-S1 _{pale}	8.11	8.11	–	0.16	–
LC1-S1 _{bulk}	7.88	7.88	–	0.31	–

Table 2 (right): Results of the carbon-content analysis.

XRD

XRD analysis results show that the samples contain calcite, quartz, and dolomite but few other minerals. The diffractograms also show minor peaks that can be attributed to feldspars, muscovite, and chlorite. Common clay minerals (e.g. illites, smectite or kaolin) were not detected. These results are consistent with those described from cave sediments in glacial environments elsewhere (Ford and Williams, 2007).

Discussion

In regions prone to glaciation, surface and subsurface features are both influenced significantly by processes associated with growth and decay of ice sheets and glaciers (Valen *et al.*, 1997; Ford and Williams, 2007). During periods of glaciation, any pre-existing caves may become connected to the sub-glacial groundwater system, commonly resulting in deposition of fine-grained clastic and organic sediments in situations with low-energy environments (Schroeder and Ford, 1983; Valen *et al.*, 1997). Passage enlargement and modifications may also occur under high-energy conditions. Whereas similar speleogenetic processes can also take place during unglaciated periods, boundary conditions and mechanisms that control the low- versus high-energy environments may differ.

Grain-size analysis results show that clastic sediments from the Greenland caves exhibit a sedimentary facies dominated by silt with some clay, but negligible quantities of sand (Table 1). The absence of coarser grain-sizes indicates that the depositional environment of the laminated sediments from Lemming Cave, as well as all the other samples from Greenland, was related to calm to stagnant hydrological conditions. Furthermore, sample LC-S1 from Lemming Cave displays distinctive laminae in the form of couplets, of a type that are commonly formed in glaciated regions (Ford and Williams, 2007). It is not yet known whether the Lemming Cave couplets are varves.

To investigate their depositional history further, the results of the grain-size analyses were compared to cumulative grain-size distribution curves for sediments found in karst caves in other glaciated areas (Fig.5). The most-closely comparable sediments are LC-S1_{dark} and finely laminated silts (Form C) from Sirijordgrotta Cave in Norway (Valen *et al.*, 1997). In the case of the Sirijordgrotta sediments, these are interpreted as glacial rhythmites (Schroeder and Ford, 1983; Larsen *et al.*, 1987) and are compared to back-flooding sediments or glacial varved sediments related to the effects of glacial damming. The grain-size distribution of LC-S1_{dark} was also found to resemble curves #13 and #16 from Fig.8.5 in Ford and Williams (2007). In the case of #13, this is described by Ford and Williams (2007) as a *terra rossa* (from southern France) that has winnowed at a depth of 30m beneath the surface. On the other hand, #16 might be windborne dust or tephra, eroded soil or reworked fluvial or lacustrine deposits.

The other sediments from Greenland (GD2-S1, GD4-S1, LC-S1_{pale}) plot similar to curves #14 and #15, with #14 interpreted the same way as #16, but #15 is attributed to the weathering of cave walls (Ford and Williams, 2007). Whereas it is possible that the homogenous silts of GD2-S1 and GD4-S1 might have originated as windblown dust (i.e. loess), eroded soil or reworked fluvial deposits, the same is unlikely to be true for the laminated LC-S1, which additionally requires an explanation for the origin of the couplets and the upward-fining. Varve-like deposits (Fig.5 #11) are common features in caves within glaciated regions (Ford and Williams, 2007). Despite this, the rhythmites from Greenland do not plot in the varved clay zone of Castleguard (Fig.5), with the Greenland samples having a higher clay content. Given that the age of these laminated deposits is not known, it is too early to draw conclusions regarding the mechanism of deposition. In the current environment, however, where the local area is not glaciated, an ice plug exists within the chamber, and this ice could have waxed and waned, resulting in localized ponding. Alternatively, if the sediments were laid down under glaciated conditions, a reasonable explanation is that the cave was connected to the sub-glacial groundwater flow and consequently recorded cyclicity within that. Alternatively, blocking and unblocking of the cave entrance by, for example, a glacier could have resulted in back-flooding of the cave.

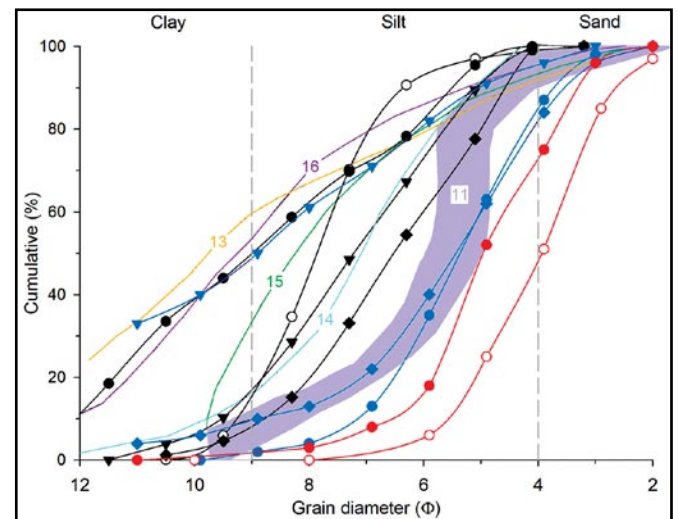


Figure 5: Cumulative grain-size distribution curves for Greenland samples versus other karst cave sediments.

Greenland samples (this study):

LC-S1_{dark} = black circles; LC-S1_{pale} = black open circles;

GD2-S1 = black triangles; GD4-S1 = black diamonds.

Finely laminated sediments from Sirijordgrotta, Norway (Valen *et al.*, 1997): Sect. V, Form A = blue circles; Sect. V, Form C = blue triangles; Sect. V, Form D, blue diamonds.

Homogenous silts from Sirijordgrotta, Norway (Valen *et al.*, 1997): Form A = red circles, red open circles.

Various curves from Ford and Williams (2007) are marked as #11 (varved clay zone in Castleguard Cave, Canada), #13, #14, #15, #16.

Conclusion

Clastic sediments were sampled from three caves in northeast Greenland. Two samples comprised homogenous silts, whereas the third was a laminated sediment containing couplets of upward-fining silt to clay. Generally, the sediments consisted of calcite, dolomite and quartz, though the clayey-silt layer contained a slightly higher level of organic carbon than the other samples.

Acknowledgements

This work was funded by the Austrian Science Fund (project no. Y 1162-N37). The Greenland government are thanked for permission to undertake this fieldwork (KNNO Expedition Permit C-19-32; Scientific Survey Licence VU-00150; Greenland National Museum and Archives 2019/01). Additionally, we thank the logistics company Polog for planning and field support; Norlandair and Air Greenland for logistics and transport; Marcel Ortler and Jasper Moernaut for assistance with the Mastersizer; Susanne Gier from the University of Vienna for carrying out the XRD analyses, Jonathan Degenfelder for preparation of Fig.1, and Ira D Sasowsky for his light reviewing of the original manuscript.

References

- Ford, T D, 2001. *Sediments in caves. (Cave Studies Series No.9)*. [Buxton: British Cave Research Association.]
- Ford, D C and Williams, P W, 2007. *Karst Hydrogeology and Geomorphology*. [Chichester: John Wiley and Sons Ltd.]
- Krinsley, D B, 1960. Limnological investigations at Centrum Sø, Northeast Greenland. *Polarforskning*, Vol.30(1/2), 24–32.
- Larsen, E, Gulliksen, S, Lauritzen, S-E, Lie, R, Løvlie, R and Mangerud, J, 1987. Cave stratigraphy in western Norway; multiple Weichselian glaciations and interstadial vertebrate fauna. *Boreas*, Vol.16, 267–292.
- Moseley, G E (Ed.), 2016. *Northeast Greenland Caves Project Expedition Report, July–August 2015*. [Innsbruck: Northeast Greenland Caves Project.]
- Moseley, G E, Barton, H A, Spötl, C, Töchterle, P, Smith, M P, Bjerkenås, S E, Blakeley, C, Hodkinson, P D, Shone, R C, Sivertsen, H C and Wright, M, 2020. Cave discoveries and speleogenetic features in northeast Greenland. *Cave and Karst Science*, Vol.47, No.2, 74–87.
- Sasowsky, I D, 2007. Clastic sediments in caves – imperfect recorders of processes in karst. 143–149 in Kranjc, A, Gabrovsek, F, Culver, D C and Sasowsky, I D (eds), *Time in Karst*. Special Publication 12, Karst Waters Institute, Leesburg, Virginia, 243pp.
- Schroeder, J and Ford, D C, 1983. Clastic sediments in Castleguard Cave, Columbia Icefields, Alberta, Canada. *Arctic and Alpine Research*, Vol.15, 451–461.
- Smith, M P and Rasmussen, J A, 2020. The geology of the Centrum Sø area of Kronprins Christian Land, northeast Greenland, and lithological constraints on speleogenesis. *Cave and Karst Science*, Vol.47(2), 60–65.
- Sun, D, Bloemendal, J, Rea, D K, Vandenberghe, J, Jiang, F, An, Z and Su, R, 2002. Grain-size distribution function of polymodal sediments in hydraulic and aeolian environments, and numerical partitioning of the sedimentary components. *Sedimentary Geology*, Vol.152(3–4), 263–277.
- Valen, V, Lauritzen, S-E and Løvlie, R, 1997. Sedimentation in a high-latitude karst cave: Sirijordgrotta, Nordland, Norway. *Norsk Geologisk Tidsskrift*, Vol.77, 233–250.
- White, W B, 2007. Cave sediments and paleoclimate. *Journal of Cave and Karst Studies*, Vol.69(1), 76–93.